FEATURES OF THE CRYSTAL STRUCTURE OF DISPERSE CARBIDES IN ALPHA TITANIUM

M. B. Ivanov, S. S. Manokhin, D. A. Nechaenko, and Yu. R. Kolobov

Investigations of disperse nonmetallic inclusions in unalloyed alpha titanium VT1-0 have been performed by using transmission electron (including scanning and high-resolution) microscopy. Characteristic electron energy losses spectroscopy has shown that these inclusions are titanium carbide particles. It has been revealed that the disperse carbides are formed in the titanium hcp matrix as a phase based on the fcc sublattice of titanium atoms. The inclusion–matrix orientation relationship corresponds to the well-known Kurdyumov–Sachs and Nishiyama–Wassermann relationships $[2\bar{1}\bar{1}0]_{\alpha} \| [011]_{\delta}$ *and* $(000\bar{1})_{\alpha} \| (1\bar{1}1)_{\delta}$.

Keywords: titanium, titanium carbide, coherent inclusions.

Titanium alloys are materials for which the potentialities of dispersion strengthening and hardening (due to precipitation of secondary phase particles from a solid solution) have not been realized. This is related to high chemical activity of titanium. Few attempts have been made to produce dispersion-hardened titanium by using particles of rare-earth metal oxides; however, these methods have not found practical use [1]. Other elements traditionally used in metallurgy to form disperse particles in metal materials (carbon and nitrogen) are considered harmful in most cases in titanium material science, including in view of the reduced probability of occurrence of nonmetallic inclusions in responsible products.

At the same time, carbon, as an alloying element, has some advantages over other impurities. When used in concentrations up to 0.1% to attain rather strong solid solution hardening, this element reduces plasticity of the material not nearly so substantially as oxygen. The main difficulty encountered in developing a technology of microalloying of titanium alloys with carbon (and other interstitial elements) is to provide its normed concentration in the alloy and a uniform distribution throughout the ingot [2].

Notwithstanding that, in popular opinion, carbon is a harmful impurity in titanium, it is widely used in practice to improve operating characteristics of many titanium alloys. Thus, the admissible content of carbon in basic "marine" alloys of types PT3V, 5V, and 37, developed at the Central Research Institute of Structural Materials "Prometey" till 90s of the last century, made 0.05–0.14% [3, 4]. In 80s, the British IMI Titaniumium Ltd. and Rolls-Royce companies have developed IMI 834 alloy, which has found wide use as a material for gas turbine engine vanes [1]. The high-temperature strength could be enhanced only by introducing 0.05–0.1 wt. % of carbon in the alloy predecessors.

An example of a beneficial effect of carbon on the properties of titanium is the nanostructured and submicrocrystalline alloy VT1-0 (commercially pure titanium) produced by methods of intense plastic deformation [5, 6]. The alloy structure produced by plastic deformation [7, 8] survives upon thermal treatments due to the retarding action of the disperse phase on the migration of grain boundaries and subboundaries. The nature of the disperse phase is now under investigation. Most of the examinations performed to the present time suggest that this phase is titanium carbide [9–11].

It has been revealed [9] that commercially pure nanostructured (NS) or submicrocrystalline (SMC) titanium possesses rather high high-temperature strength, higher than that of the metals with close melting points (e.g., nickel).

REC "Nanostructured Materials and Nanotechnologies" of Belgorod State University, Belgorod, Russia, e-mail: Nechaenko @bsu.edu.ru; Kolobov @bsu.edu.ru.

TABLE 1. Chemical Compsition of Titanium VT1-0, wt. % (Ti Base)

OST1 90013-81 requirement	Al	C	N_2	Fe	Si	H_2	O_2
	≤0.70	≤0.07	≤0.04	≤0.25	≤0.10	≤0.006	≤0.20
Actual value	0.010	0.004	0.003	0.12	0.002	0.0008	0.143

The high high-temperature strength ensures that titanium rods and profiles intended for manufacturing implants can be annealed for removing first kind stresses (macrostresses), makes the metal structure tolerant to climatic actions and sterilizations, and guarantees high long-term performance of the products in a human body.

However, the question of the reasons for the high thermal stability of commercially pure titanium in the NS and SMC states still remains open. It is obvious that the potentialities of optimization of the material properties by using both thermal treatment and microalloying, including with maximum permissible concentrations of poorly soluble impurities, are not exhausted. It is supposed that the presence of poorly soluble impurities, such as carbon, is responsible for the good points of SMC and NS titanium.

In the present study, the method of transmission electron (including scanning and high-resolution) microscopy was used to examine disperse nonmetallic inclusions in unalloyed titanium VT1-0 for their phase and element composition and to determine their orientation relationship with the metal matrix.

TEST MATERIAL AND INVESTIGATION PROCEDURE

Unalloyed titanium VT1-0 (the chemical composition is given in Table 1) subject to 50% strain by flat cold rolling was used for investigations. The material was annealed at a temperature of 1193 K (above the polymorphic transformation temperature (PTT) in the beta-phase range) for 1 h and then cooled to 1143 K (temperature below PTT) together with the furnace. The samples were soaked at 1143 K for 0.5 h and then water quenched.

The microstructure of the samples was examined by methods of optical metallography (Olympus GX71 microscope) and transmission electron microscopy (TEM) (Tecnai G2 F20 S-TWIN microscope).

To prepare metallographic sections of the samples for optical microscopy, grinding papers with different grit sizes were used. Finish grinding was performed with water-based diamond suspension. At the final stage, the metallographic sections were electropolished or etched. The electrolyte composition was 60% H_2SO_4 – 30% HNO_3 – 10% HF; the etchant consisted of 95% H_2O and 10% HF.

The following transmission electron microscopy imaging methods were used: the light-field and dark-field contrast method (i); high-resolution electron microscopy (ii); dark-field scanning transmission electron microscopy (STEM) (with detection of high-angle scattered electrons) (iii), and light-field STEM (with detection of undiffracted and unscattered electrons).

To prepare thin foils, jet polishing (TenuPol-5 machine) was used. The electrolyte composition was 20% $HClO_4$ + 80% CH_3CO_2H.

Element analysis was performed by the method of energy dispersive x-ray microanalysis with the use of an EDAX attachment to the transmission electron microscope and Genesis Microanalysis Software in the STEM mode and by the method of characteristic electron energy losses (CEEL) spectroscopy. The CEEL spectra have been obtained at an accelerating voltage of 200 kV in a converging beam (nanoprobe) mode (the beam diameter was 10 nm) with the use of a postcolumn sector-type filter (Gatan 860 GIF 2001) allowing 0.7 eV resolution and have been analyzed with the use of the Digital Micrograph v.1.8 software package (background subtraction and deconvolution).

RESULTS AND DISCUSSION

Examination of the microstructure of titanium VT1-0 after staged annealing from 1193 to 1143 K and quenching from 1143 K has revealed a lamellar coarse-grained structure in the material (Fig. 1*a*).

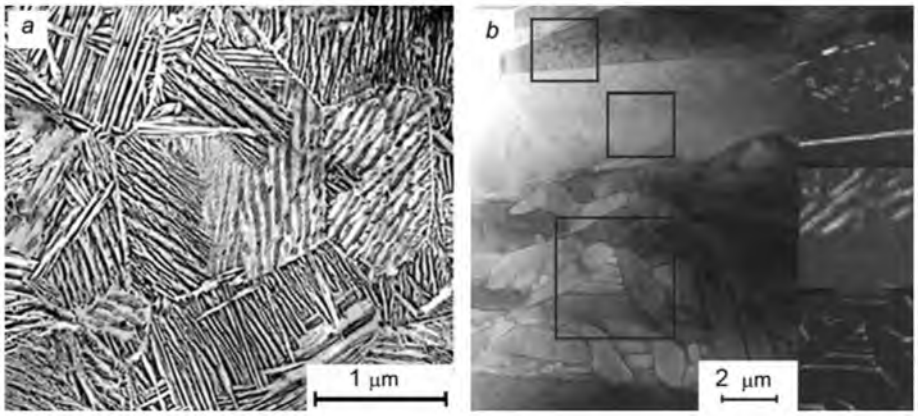

Fig. 1. Microstructure of titanium VT1-0 annealed at 1193 T and subsequently furnace cooled to 1143 K, soaked for 0.5 h, and water quenched: optical metallography (*a*) and light-field STEM (*b*). Insets: Distribution of iron in the image squared regions (STEM microanalysis).

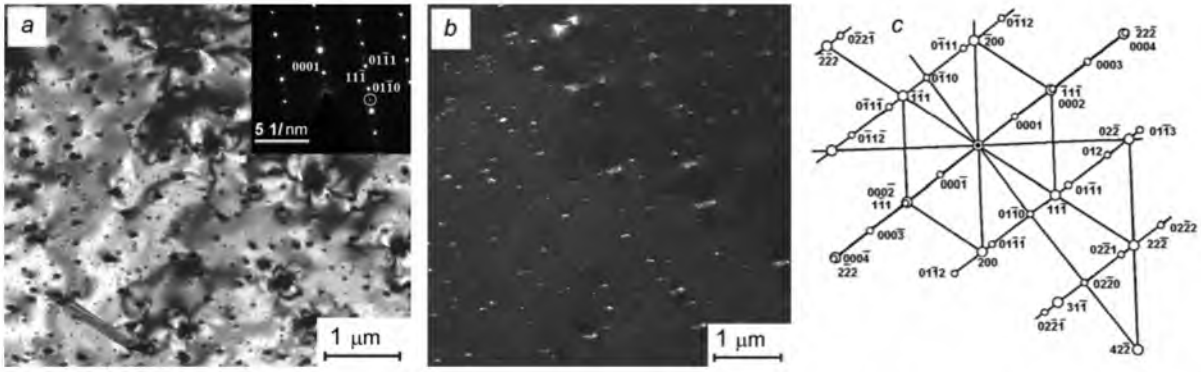

Fig. 2. Carbide particles in titanium VT1-0 homogenized at a temperature higher than the temperature of polymorphic transformation, furnace-cooled to the α-phase, and quenched: light-field image (inset: diffraction pattern); dark-field image in an extra reflection (circled in the diffraction pattern) (*b*), and the interpretation of the diffraction pattern showing the hcp–fcc orientation relationship.

The distribution of iron, according to thin foil microanalysis (STEM) is given in Fig. 1. When the material is cooled from a temperature higher than the polymorphic transformation temperature, the impurity iron, being the stabilizer of the β-phase, is redistributed by diffusion, resulting in the formation of thin β–phase layers between α-phase plates; it is also observed in the bulk of large α-phase plates in the form of extended particles of rather large size (from several parts of a micrometer to several micrometers).

The β-phase formed along the boundaries of the α-plates and in their thriple joints experiences martensitic transformation on quenching from 1143 K. Thus, the bulk α-phase is free from iron, both dissolved and bound in the disperse inclusions (β-phase, iron intermetallides).

Nevertheless, in the α-phase grains well oriented in relation to the electron beam, strain contrast from disperse inclusions (contrast from the stress field) is observed. The diffraction pattern shows, irrespective of the region under analysis, type {0001} reflections of the fcp titanium lattice forbidden by the structure geometric factor are observed. In addition, if the α-phase is precisely oriented, extra reflections of inappreciable intensity are detected along the axes of the $\langle 2\bar{1}\bar{1}0 \rangle$ zone (Fig. 2*a*). In this case, disperse particles can be seen in great numbers in the dark field image taken from an extra reflection (see Fig. 2*a*).

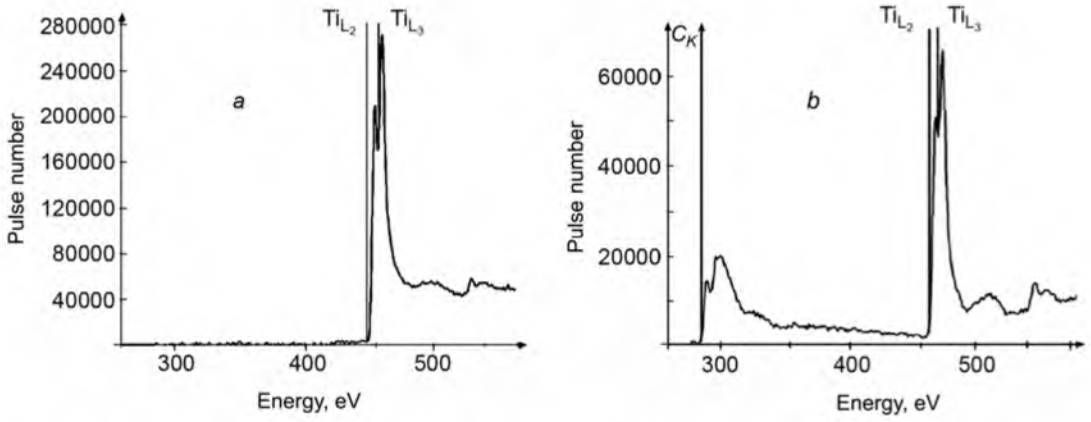

Fig. 3. Spectra of characteristic electron energy losses for the α-phase (*a*) and for the titanium carbide particle presented in Fig. 2 (*b*).

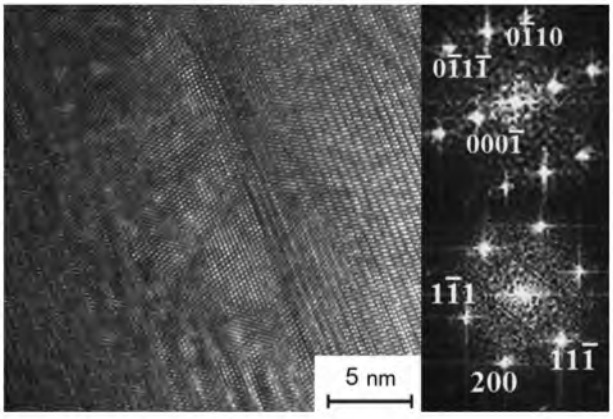

Fig. 4. Image of a titanium carbide particle taken after its homogenization at a temperature higher than the temperature of polymorphic transformation, furnace-cooling to the α-phase, and quenching, taken by using high-resolution transmission electron microscopy, and the Fourier transform of image fragments (from top tobottom) for the matrix and the particle.

The CEEL spectroscopy data for the inclusions suggest that they are particles of titanium carbides (δ-phase). This is evidenced by the intense absorption peaks in the *K*-line of carbon (Fig. 3) that are not inherent in the titanium. The particles contain no elements other than carbon and titanium (at least in contents exceeding a few percents corresponding to the limit of detection by CEEL spectroscopy).

High-resolution transmission electron microscopy has shown that the particles have the fcc sublattice of titanium atoms (Fig. 4). This has been revealed by analyzing the fast Fourier transform (FFT) data for high-resolution images of the particles taken at the $[2\bar{1}\bar{1}0]$ axis of the matrix zone. It should be noted that the particles and the matrix have the following orientation relations: $(000\bar{1})_\alpha \| (1\bar{1}1)_\delta$ for the planes and $[2\bar{1}\bar{1}0]_\alpha \| [011]_\delta$ for the directions. The lattice parameters of the particles, according to FFT, are about 2.4, 2.1, and 1.5 Å, respectively. They coincide with the well-known lattice parameters of titanium carbide TiC [12]. The stoichoimetry of the particles could not be found unambiguously because of their small sizes and, hence, low reflectivity.

It was observed that titanium VT1-0 homogenized at 1193 K, furnace-cooled to the quenching temperature, and quenched from 1143 K contained titanium carbides with the fcc sublattice of titanium atoms. The high-resolution TEM

data and diffraction patterns unambiguously point to the orientation relationships $[2\bar{1}\bar{1}0]_\alpha \| [011]_\delta$ and $(000\bar{1})_\alpha \| (1\bar{1}1)_\delta$ that are sketched in Fig. 2*c*. Thus, carbide is formed in the hcp matrix as a massive stacking fault on close-packed planes.

The boundary between the matrix and a particle of small size is coherent (over close-packed planes), and this results in high elastic stresses both in the particle and in the matrix due to different periods of translation along the boundary in the matrix and in the particle. This gives rise to strain contrast by which particles are detected.

Disperse carbon-base precipitates in SMC and NC titanium VT1-0 were first analyzed in the study presented elsewhere [10]. Electron diffraction patterns showed extra reflections located halfway between titanium (0002) reflections. Similar extra reflections appear in recrystallized grains of SMC titanium on annealing (773 K). Simultaneously, disperse coherent phase precipitates are observed which are visible due to strain contrast. Larger precipitates are located on and near grain boundaries. The reflections related to TiC carbides are not observed after annealing at 773 K. It has been supposed [10] that the observed particles are precipitates of a carbon-base metastable phase, as carbon is (at 773 K) the least solvable interstitial impurity in titanium. The solvability of carbon in the α-phase increases as the temperature is increased to 1073–1123 K. In the experiment described in Ref. 10, a sample of titanium VT1-0 was quenched in vacuum from 1073–1123 K. Electron diffraction patterns have shown that after quenching, the titanium structure contained only lamellar precipitates of TiC titanium carbide. Thereafter, the sample was aged at 773 K for 1 h. The structure of the aged sample contained disperse coherent phase precipitates, causing strain contrast, and TiC particles, which produces reflections corresponding to the lattice of TiC in electron diffraction patterns. Dark-field examination in reflections of TiC has revealed no luminescence of disperse precipitates, suggesting that a metastable phase precipitated in aging, whereas large TiC particles that were present in the quenched state survived.

The occurrence of type (0001) extra reflections, forbidden by the structural factor for α-Ti, is interpreted [10] based on a model according to which the precipitated carbon is located in octahedral interstices between two adjacent planes of the titanium hcp lattice base. It is expected that the next interstitial plane will be free from carbon atoms and then the spacing between its adjacent planes of titanium will be shorter. As a result, a modulation of interplanar spacings with a period "c" will arise that will partially moderate the increase in precipitate volume due to the increased concentration of carbon atoms. The modulation is responsible for the appearance of type (0001) reflections forbidden by the structural factor for α-Ti in electron diffraction patterns. In addition, the planes filled with carbon atoms with period "c" can also be responsible for the appearance of (0001) reflections. As a plane of interstices is completely filled with carbon atoms, a type Ti_2C stoichiometric compound arises. The phase formed at low temperatures is metastable and, at high temperatures, it is replaced by stable TiC precipitates.

However, the results of the present study allow some refinements to be made. We have actually detected disperse precipitates of carbides, namely fcc carbide rather than a metastable phase with hcp lattice, and have found a precise orientation relationship between the matrix and a particle. If the particle is small in volume, its reflectivity is insignificant, and its small thickness (of the order of several nanometers) is responsible for an additional broadening of diffraction peaks. As a result, the particle plays more likely the part of a stacking fault in the formation of a diffraction pattern, as can be judged by the appearance of (0001) maxima that are forbidden for an hcp lattice. In this case, the diffraction pattern for the particle is indiscernible, in particular if the foil is oriented not along the axis of the particle region. As in the experiment presented in Ref. 10, disperse particles were not observed in dark-field examinations of the reflections of large TiC particles whose orientation relationship with the matrix is different from that for disperse particles. Actually, as carbides increase in size, they should loose coherence with the matrix due to the difference in the period of translation along the boundary between the matrix and the particle. Most likely, they are not separated from the matrix by a high-angle boundary and their orientation is more profitable than that observed in the present study.

The relationship $[2\bar{1}\bar{1}0]_\alpha \| [011]_\delta$ revealed is well known in the literature as the Kurdyumov–Sachs or Nishiyama–Wassermann orientation relationship. For titanium alloys, it is more often referred to as the Blackburn relationship [1] that describes the decay of a solid solution in titanium aluminide: $\alpha \rightarrow \alpha_2 + \gamma$. By analogy, it can be supposed that the particles nucleate and grow by the diffusion mechanism. Initially, a shear mechanism of the formation of an hcp phase in titanium aluminides was supposed [13]. However, subsequently these suppositions were seriously criticized with the use of the results of earlier studies [14] where the diffusion decay of a supersaturated solid solution of aluminum in argentum with precipitation of γ-$AlAg_2$ was evidenced. Subsequently, Aindow and Pond [15] cited

proofs for the diffusion mechanism of the formation of fcc inclusions in an hcp matrix due to a conservative motion of partial dislocations along interphase boundaries (based on the topological theory of defects of interior interfaces).

Thus, it can be supposed that particles grow or are dissolved due to the directional diffusion of carbon in the hcp lattice of titanium in the stress field of the growing particle. The growth/dissolution is not accompanied by migration of the interphase boundary in classical representation, but is determined by the conservative motion of partial dislocations responsible for the propagation of a massive stacking fault (fcc in hcp). The nucleation of a particle can be described as the formation of Guinier–Preston zones with a local nonuniform distribution of carbon, resulting in destabilization of the lattice (development of shear instability) followed by the formation of a new partially coherent phase. As several stable phases can be formed if the carbide composition is nonstoichiometric (carbon deficiency characteristic of the initial stages of decay of a solid solution) [16], the nucleation of a certain phase which is associated with a minimum energy of the system in view of the excess energy of the phase boundary related to the coherence of lattices and to elastic stresses, both in the particle and in the surrounding matrix, will be most energy efficient. Thus, initially the formation of a metastable hcp phase is possible which then undergoes transformation into fcc carbide. However, it should be noted that, according to original data, the stage of decay of a solid solution of carbon in hcp titanium proceeds almost completely even at room temperature due to the high mobility of carbon. Most likely, the decay of the solid solution of carbon in titanium at room temperature in the earlier experiment [10], where STEM and high resolution TEM were not used, could not be observed for technical reasons.

CONCLUSION

As a result of quenching of alpha titanium VT1-0 from a temperature close to the temperature of polymorphic transformation, disperse nonmetallic inclusions of lamellar morphology with nanometer sizes are formed. By using the method of characteristic electron energy losses spectroscopy it has been shown that these inclusions are titanium carbide particles. Therefore, it is impossible to fix a solid solution of carbon in alpha-titanium at room temperature because of the high diffusion mobility of carbon.

It has been revealed that the disperse carbides are formed in the hcp matrix of titanium as a phase based on the fcc sublattice of titanium atoms. The inclusion–matrix orientation relationship corresponds to the well-known Kurdyumov–Sachs, Nishiyama–Wassermann, and Blackburn relationships: $[2\bar{1}\bar{1}0]_\alpha \| [011]_\delta$ and $(000\bar{1})_\alpha \| (1\bar{1}1)_\delta$. The boundary between the hcp matrix and a small-size fcc particle is partially coherent relative to the close-packed (0001) planes of the base, resulting in intense stresses both in the particle and in the surrounding matrix.

The work was supported in part by the Federal Purpose-Oriented Program “Scientific and Pedagogical Staff of the Innovative Russia” for 2009–2013 (State contracts Nos. 14.740.11.0705 and 16.740.11.0025) and by the Analytic Departmental Purpose-Oriented Program “Development of the Scientific Potential of the Higher School” (project No. 2.1.2/1061) with the use of the Diagnostics of Structure and Properties of Nanomaterials analytical equipment of the Centre of Collective Using Research Equipment of Belgorod State University.

REFERENCES

1. Christoph Leyens and Manfred Peters, Titanium and Titanium Alloys. Fundamentals and Applications, WILEY-VCH Verlag, Weinheim (2003).
2. E. A. Karasev, A. S. Kudryavtsev, and L. A. Machishina, Titanium, No. 3/4 (7/8), 3–5 (1995).
3. A. L. Bereslavskii, S. A. Emel’anov, V. M. Maksimov, and L. A. Machishina, *Ibid.*, 15–17.
4. D. A. Panotskii and A. L. Bereslavskii, *Ibid.*, No. 1 (18), 20–23 (2006).
5. Yu. R. Kolobov, Rossiiskie Nanotekhnologii, No. 11/12, 19–31 (2009).
6. M. B. Ivanov, Yu. R. Kolobov, E. V. Golosov, *et al.*, *Ibid.*, No. 3/4 (2011).
7. Yu. R. Kolobov, M. B. Ivanov, E. V. Golosov, and A. V. Penkin, Method of Production of a Submicrocrystalline Structure in Unalloyed Titanium, Patent of the Russian Federation No. 2389568, priority of 29.12.2008 [in Russian].

8. M. B. Ivanov, A. V. Penkin, Yu. R. Kolobov, *et al.*, Deform. Razrushenie Mater., No. 9, 13–18 (2010).
9. Yu. R. Kolobov, O. A. Kashin, E. E. Sagymbaev, *et al.*, Russ. Phys. J., No. 1, 71–78 (2000).
10. L. S. Bushnev, L. V. Chernova, and N. V. Girsova, Fiz. Met. Metalloved., **92**, No. 3, 44–51 (2001).
11. Yu. R. Kolobov, A. G. Lipnitskii, M. B. Ivanov, and E. V. Golosov, Kompozity & Nanostruktury, No. 2, 5–32 (2009).
12. The Landolt-Börnstein database. http:// www.springermaterials.com/navigation/index.html
13. Y. Q. Sun, Phil. Mag. Lett., **78**, No. 4, 297–305 (1998).
14. J. Kwarciak, J. Thermal Analysis, **30**, 177–185 (1985).
15. M. Aindow, T. T. Cheng, C. Lin, *et al.*, Inter. Sci., No. 12, 293–302 (2004).
16. A. G. Lipnitskii, D. A. Aksenov, Yu. R. Kolobov, Russ. Phys. J., No. 10, 1047–1051 (2009).